Bull. Chem. Soc. Ethiop. **2024**, 38(3), 671-684.
DOI: https://dx.doi.org/10.4314/bcse.v38i3.10

ISSN 1011-3924
Printed in Ethiopia
Online ISSN 1726-801X

PREPARATION, SPECTROSCOPIC AND ANTICANCER INVESTIGATIONS OF METAL-DRUG COMPLEXES ASSOCIATED BETWEEN FLUMEQUINE ANTIBIOTIC DRUG WITH LANTHANUM(III), SAMARIUM(III) AND TERBIUM(III) CHLORIDE

Abeer A. El-Habeeb[1], Mohamed Y. El-Sayed[2], Ibrahim M.A. Alatawy[2] and Moamen S. Refat[3*]

[1]Department of Chemistry, College of Science, Princess Nourah bint Abdulrahman University, P.O. Box 84428, Riyadh 11671, Saudi Arabia
[2]Chemistry Department, College of Science, Jouf University, Sakaka 2014, Saudi Arabia
[3]Department of Chemistry, College of Science, Taif University, P.O. Box 11099, Taif 21944, Saudi Arabia

(Received December 18, 2024; Revised February 8, 2024; Accepted February 15, 2024)

ABSTRACT. Flumequine ligand (FLQ) metal complexes of the $[M(FLQ)_2(Cl)(H_2O)].nH_2O$ type, where M are (La(III), Sm(III), and Tb(III)) and FLQ is flumequine have been synthesized. The FLQ metal complexes could be prepared using MCl_3 : flumequine in stoichiometry of 1:2 in *situ* bidentate chelation. The characterization of FLQ complexes obtained have been done using elemental analyses (%C, %H and %N), molar conductivity (Λ_m), infrared spectroscopy (FTIR), electronic spectra (UV-Vis), thermal analysis (TGA), and physicochemical techniques such as X-ray powder diffraction (XRD), scanning electron microscopy (SEM), and energy dispersive X-ray (EDX) measurements at room temperature. Accordingly, these complexes are indicative of an octahedral coordination structure. Flumequine ligand has a bidentate fashion through the oxygen atoms of carbonyl (quinolone) and carboxylic groups. The findings demonstrated the anti-cancer efficacy of these compounds against HepG-2 and MCF-7 cancer cell lines at extremely low doses of up to 58.2 µg/mL. The La(III) complex was shown to have the highest selectivity against cancer cells in comparable with both samarium and terbium(III) complexes.

KEY WORDS: Flumequine, Lanthanide metal ions, Ftir, EDX, Complexation, Anticancer activity

INTRODUCTION

Quinolones, also known as 4-quinolones or quinolones carboxylic acids, are a class of synthetic antibacterial drugs [1-3] that are frequently used to treat a variety of infections [4, 5]. Quinolones effectively impede DNA replication. Antibiotics can enter the environment through veterinary and human routes, primarily through the soil-dwelling of manure and human excretions. Furthermore, several studies have demonstrated that antibiotics frequently do not get removed during wastewater treatment and do not break down naturally in the environment [6, 7]. A synthetic first-generation quinolone molecule is called flumequine (Figure 1). Because it is chiral and has a racemic mixture as a ligand, flumequine is a very successful treatment for UTIs [8]. It is mostly used in veterinary medicine to treat illnesses in animals brought on by a variety of Gram-negative bacteria [9-11]. Many studies have been conducted on copper, one of the most intriguing biometals [12, 13] because of its biological significance and possible synergistic activity with medications [14, 15]. Numerous biological effects, including anticancer [16, 17], antioxidant [18, 19], antibacterial [20-22], and antifungal [23], have been demonstrated by copper(II) complexes with a variety of medicines.

Much work has been done in the field of lanthanide coordination chemistry in recent years, and it has been found that these compounds have special photophysical qualities that are very useful in a variety of practical applications, including plastic lasers, materials science, fluorescent biology sensors, and catalysis. The lanthanide complexes' unique electronic configuration is

*Corresponding authors. E-mail: moamen@tu.edu.sa ; msrefat@yahoo.com

responsible for a number of properties, including their reduction behavior and fluorescence, which make them extremely valuable in the medical field for diagnosis and treatment. These include biomedical examinations like magnetic resonance imaging, anti-inflammatory, antimicrobial, antifungal, and chemotherapy for cancer prevention [24, 25]. Because lanthanide compounds can attach to DNA more efficiently by hydrogen bonds or the hydrolyzed mode than transition metal complexes can, they are a promising agent in the field of medical chemistry [26]. These are mostly caused by platinum's suitability as a hefty core metal atom for biological systems. Therefore, in order to prevent the possible toxicity, new anti-tumour metal complexes with more amiable center metal atoms must be developed. La(III) complexes have been the subject of much research among other metal complexes because of their higher physiological activity and decreased toxicities following ligand coordination. Most people consider rare earth cations (Ln^{III}) to be a type of pseudo-calcium II ions. This makes sense given that they have comparable environmentally beneficial qualities to calcium(II) [27]. As a result, rare earth cations are frequently utilized in various chemical fertilizers and feed additives that may aid increase cattle growth rates or grain yields. Rare earth cations can form complexes with specific bioactive ligands that demonstrate matching pharmacological properties and diverse applications, particularly in cancer diagnostics [28-29]. This results in a higher stability and activity compared to ligands or rare earth cations alone [30]. According to these investigations, rare earth complexes have a lot of potential for use in biomedical applications.

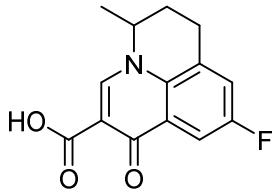

Figure 1. Flumequine structure.

To improve the effectiveness of medications, we have concentrated our research on divalent and trivalent metal ions complexes with various drugs. We have found that these complexes may have more produced biological qualities than the drugs alone. Flumequine, a synthetic first-generation quinolone, shares structural similarities with ofloxacin or nalidixic and oxolinic acids [31]. Flumequine has been shown to have activity against certain Gram-positive and Gram-negative pathogens in addition to being a highly efficient treatment for urinary tract infections [32]. The anti-tumor activity of flumequine in metal complexes with Ni(II) [33], Cu(II) [34], zinc(II) [35], and Co(II) [36] has been assessed through structural characterization. To determine the coordination mode of flumequine with lanthanide metal ions, we report here the synthesis and characterizations of various novel lanthanide metal(III) complexes (lanthanum, samarium, and terbium) with flumequine ligand. By measuring the minimum inhibitory concentration (MIC) and half-minimum inhibitory concentration (IC50) against four Gram-positive and Gram-negative bacteria, flumequine complexes were found to have antibacterial activity. Furthermore, the disclosed complexes' anticancer efficacy was tested against the HepG-2 and MCF-7 cell lines.

EXPERIMENTAL

Materials and instrumentations

The analytical reagent grade materials utilized in this investigation were flumequine, lanthanium(III) chloride heptahydrate, samarium(III) chloride hexahydrate, terbium(III) chloride hexahydrate, and ammonium hydroxide. These materials were obtained commercially from

Aldrich without undergoing prior purification. Vario EL Fab. CHNS has been used for the elements of carbon, hydrogen, and nitrogen. The thermal gravimetric analysis method was used to measure the water content and the percentages of metal ions. Using newly made solutions, the molar conductances of 10^{-3} M solutions in DMSO solvent were measured at room temperature using a replica of a HACH conductivity meter. Using a Bruker infrared spectrophotometer, the synthesized mixed ligand complexes' FTIR spectra were obtained in the 400–4000 cm^{-1} range. The Unicam UV/Vis spectrometer was used to scan the electronic spectra using DMSO as a solvent in the 200–800 nm range. Thermal analyzers made by Shimadzu, model TGA-50H, were used to measure thermogravimetric analysis (TGA). A single loose top loading platinum sample pan was used for all tests, which were carried out in an environment of nitrogen at a flow rate of 30 mL/min and a heating rate of 10 °C/min for a temperature range of 25–600 °C. Using an acceleration voltage of 25 kV, a Jeol Jem-1200 EX II Electron microscope was used to produce SEM pictures and EDX spectra of synthesized FLQ complexes. Using an X Pert Philips X-ray diffractometer, the samples' X-ray diffraction (XRD) patterns were captured. $CuK_{\alpha 1}$ radiation was used to obtain all the diffraction patterns, and a graphite monochromator was used to scan at a rate of 0.02 °/min.

Preparation of flumequine La, Sm, and Tb(III) complexes

The three lanthanide chlorides' flumequine complexes were made by refluxing a mixture containing 1 mmol (0.372 g) of $LaCl_3.7H_2O$, 1 mmol (0.373 g) of $TbCl_3.6H_2O$, 1 mmol (0.365 g) of $SmCl_3.6H_2O$, and 2 mmol of flumequine (0.523 g) ligand in 95% methanol solvent on a hotplate for two hours at 60 ºC. The mixtures were then neutralized at pH 7-9 with a few drops of alcoholic ammonia solution. The mixes were left at the same volume for the entire night, at which point the precipitates started to form right away. After filtering off the precipitations, a few drops of diethyl ether were added, and the mixture was then dried in a vacuum desiccator over anhydrous $CaCl_2$. The separated solid products had yields between 75 and 80 percent.

Anti-cancer experiment

Mammalian cell lines: the VACSERA Tissue Culture Unit provided the human breast cancer cell line MCF-7 and the human hepatocellular carcinoma cell line HepG-2. Chemicals used: Sigma (St. Louis, Mo., USA) provided the trypan blue dye, crystal violet, and dimethyl sulfoxide (DMSO). Purchased from Lonza were fetal bovine serum, DMEM, RPMI-1640, HEPES buffer solution, L-glutamine, gentamycin, and 0.25% Trypsin-EDTA. The composition of the 0.5% (w/v) crystal violet stain is 50% methanol and 0.5% crystal violet. The mixture is then brought up to volume with ddH_2O (Double distilled water (abbreviated "ddH_2O" or "Bidest. water") and filtered using Whatmann No. 1 filter paper.

Cell line propagation

The cells were cultured in Dulbecco's modified Eagle's medium (DMEM), which was enhanced with 50µg/mL of gentamycin, 10% heat-inactivated fetal bovine serum, 1% L-glutamine, and HEPES buffer. Every cell was cultivated twice a week and kept at 37 ºC in a humidified environment with 5% CO_2.

Evaluation of cytotoxicity by viability assay: To perform the cytotoxicity experiment, 100µl of growth media was added to each well of a 96-well plate, with 1×104 cells per well. A fresh medium was added 24 hours after sowing, with varying concentrations of the test sample. Confluent cell monolayers were distributed into 96-well flat-bottomed microtiter plates (Falcon, NJ, USA) using a multichannel pipette, and serial two-fold dilutions of the investigated chemical compound were added. The microtiter plates were incubated for twenty-four hours at 37ºC in a

humidified incubator containing 5% CO_2. For every concentration of the test sample, three wells were utilized. DMSO and/or test sample were not used during the incubation of control cells. The experiment was shown to be unaffected by the small amount of DMSO (maximum 0.1%) in the wells. A colorimetric approach was used to determine the viable cell yield following a 24-hour incubation period at 37 °C.

To sum up, after the incubation period ended, the media were removed and each well received a minimum of 30 minutes of addition of the 1% crystal violet solution. After the stain was eliminated, the plates were thoroughly cleaned with tap water to eliminate any remaining residue. After adding 30% glacial acetic acid to each well and properly mixing them, the plates were gently shaken on a Microplate Reader (TECAN, Inc.) to measure the absorbance of the material using a test wavelength of 490 nm. To account for background absorbance found in wells without additional stain, all values were adjusted. In the absence of the investigated substances, treated samples were contrasted with the cell control. Every experiment was run in triplicate. Every investigated compound's cytotoxic effect on cells was calculated. The number of viable cells was ascertained by measuring the optical density using a microplate reader (SunRise, TECAN, Inc., USA). The percentage of viability was computed as [(ODt/ODc)] × 100%, where ODt represents the mean optical density of wells treated with the tested sample and ODc represents the mean optical density of untreated cells. The survival curve of each tumor cell line following treatment with the designated substance is obtained by plotting the relationship between remaining cells and drug concentration. Using Graphpad Prism software (San Diego, CA, USA), the 50% inhibitory concentration (IC_{50}), or the concentration needed to elicit harmful effects in 50% of intact cells, was determined using graphic plots of the dose response curve for each conc. [37, 38].

RESULTS AND DISCUSSION

Microanalytical and molar conductance values

The following chemical equations can be used to illustrate the formation of the Metal-Drug complexes of La(III), Sm(III), and Tb(III) metal ions utilizing flumequine as a bidentate ligand:

i- $LaCl_3.7H_2O+2FLQ+2NH_4OH \rightarrow [La(C_{28}H_{22}ClF_2N_2O_6)(Cl)(H_2O)].3H_2O+2H_2O+2NH_4Cl$

ii- $SmCl_3.6H_2O+2FLQ+2NH_4OH \rightarrow [Sm(C_{28}H_{22}ClF_2N_2O_6)(Cl)(H_2O)]+2H_2O+2NH_4Cl$

iii- $TbCl_3.6H_2O+2FLQ+2NH_4OH \rightarrow [Tb(C_{28}H_{22}ClF_2N_2O_6)(Cl)(H_2O)].2H_2O+2H_2O+2NH_4Cl$

(where FLQ = $C_{14}H_{12}FNO_3$ is flumequine)

The ligand flumequine FLQ chelates to La(III), Sm(III), and Tb(III) metal chlorides to produce the $[La(C_{28}H_{22}ClF_2N_2O_6)(Cl)(H_2O)].3H_2O$, $[Sm(C_{28}H_{22}ClF_2N_2O_6)(Cl)(H_2O)]$, and $[Tb(C_{28}H_{22}ClF_2N_2O_6)(Cl)(H_2O)].2H_2O$ complexes. The stable $[M(C_{28}H_{22}ClF_2N_2O_6)(Cl)\ (H_2O)].nH_2O$ complexes are generally synthesized, these are dissolved in common organic solvents like DMSO and DMF, but insoluble in water and alcohols. The color of each complex ranges from pale yellow to yellow. According to Table 1, the solid complexes have a tight connection between the metal and the ligand, making them thermally stable. The metal complexes' microanalytical analysis results are attributed to their general formulation, which is $[M(C_{28}H_{22}ClF_2N_2O_6)(Cl)(H_2O)].nH_2O$ complexes (Table 1). The molar conductance values of complexes in dimethyl sulfoxide (DMSO) at concentrations of 10^{-3} M fall within the range of $\Lambda m = 18–25\ \Omega^{-1}mol^{-1}cm^{-1}$, suggesting that they are not electrolytic [39]. This can be attributed to the absence of Cl ions outside of the coordination sphere. The elemental analysis, as well as the molar conductance data, are convenient with the suggested structures of $[M(FLQ)_2(Cl)(H_2O)].nH_2O$ complexes that can be formulated as $[La(FLQ)_2(Cl)(H_2O)].3H_2O$, $[Sm(FLQ)_2(Cl)(H_2O)]$, and $[Tb(FLQ)_2(Cl)(H_2O)].2H_2O$ (Figure 2). The coordination modes of FLQ ligand towards

lanthanum(III), samarium(III), and terbium(III) metal ions were investigated dependent on the infrared, molar conductance, and thermal analyses.

Table 1. Microanalytical and physical values of $[M(FLQ)_2(Cl)(H_2O)].nH_2O$ complexes.

Compounds	Colour	m.p/°C	Λ_m	Elemental analysis, % found % (calcd.)				
				C	H	N	Cl	M
La(III) complex	Yellow	>300	25	43.54 (43.81)	3.78 (3.91)	3.61 (3.65)	4.61 (4.63)	17.97 (18.11)
Sm(III) complex	Pale Yellow	>300	22	46.23 (46.41)	3.29 (3.31)	3.80 (3.87)	4.77 (4.90)	20.43 (20.67)
Tb(III) complex	Yellow	>300	18	43.44 (43.69)	3.59 (3.64)	3.54 (3.64)	4.56 (4.62)	20.60 (20.77)

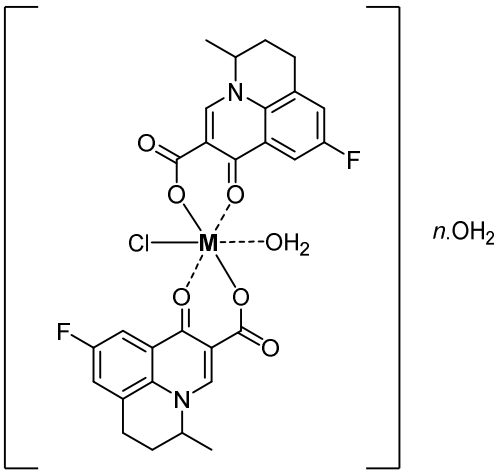

Figure 2. Suggested structures of $[M(C_{28}H_{22}ClF_2N_2O_6)(Cl)(H_2O)].nH_2O$ complexes, where M = La(III) with n = 3; Sm(III) with n = 0 and Tb(III) with n = 2.

Infrared and UV–Vis spectra

The infrared spectra of the free flumequine and its complexes with the lanthanides ions La(III), Tb(III) and Sm(III) are displayed in Figure 3A-C. The major infrared frequencies of these compounds can be assigned and summarize in Table 2. The flumequine molecule had several characteristic vibrational modes on the IR spectrum. The bands at 1725 cm^{-1} and 1267 cm^{-1} are attributed to stretching vibration motions of $\nu(C=O)_{carboxylic}$ and $\nu(C\text{-}O)_{carboxylic}$, respectively of the carboxylic group of flumequine. These two bands have been replaced by two very strong characteristic bands within the range of 1569-1598 cm^{-1} and 1374-1384 cm^{-1} which are assigned to antisymmetric $\nu_{asym}(C=O)$ and symmetric $\nu_{sym}(C=O)$ stretching vibration of carboxylato group. The values of $\Delta = \nu_{asym}(C=O) - \nu_{sym}(C=O)$ are present in the range of 195-223 cm^{-1} suggested a monodentate coordinate mode regarding carboxylic group. The band slightly shifted from 1617 cm^{-1} to 1627-1646 cm^{-1} concerning $\nu(C=O)$ pyridine vibration explained a chelate coordination mode of flumequinato ligand to lanthanide metal ions(III) *via* the pyridone oxygen and carboxylato oxygen. The new bands observed in the infrared spectra for all complexes within the range of 409-488 cm^{-1} can be assigned to $\nu(M\text{-}O)$ bands [40-42].

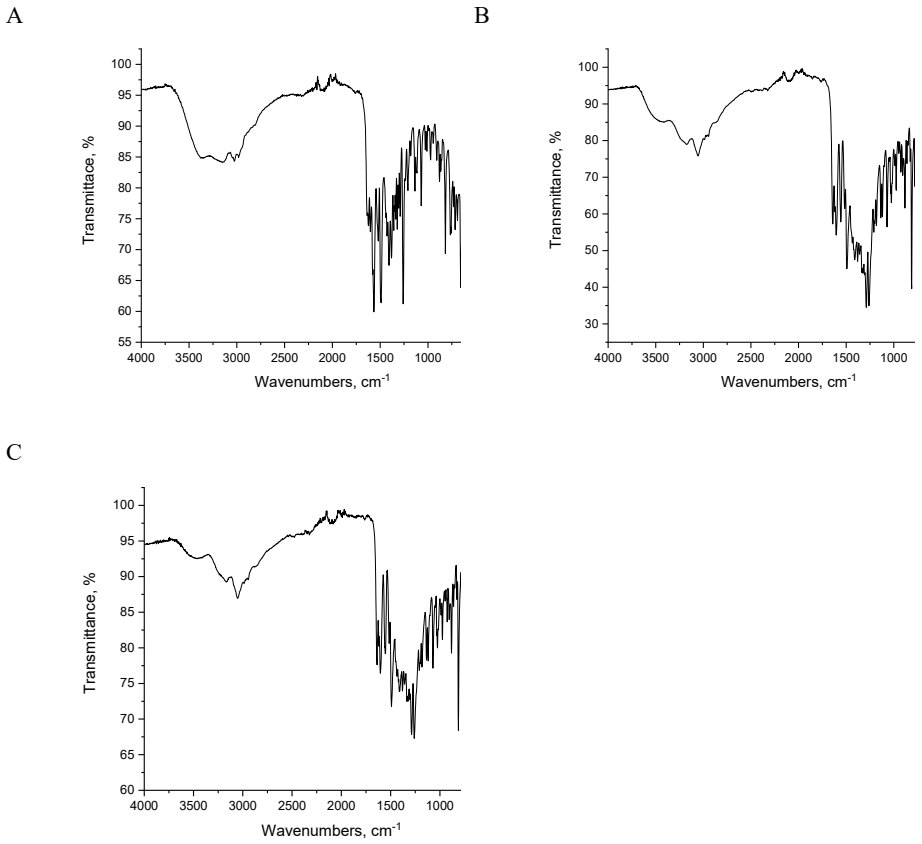

Figure 3. Infrared spectra of (A): La(III) flumequine, (B): Tb(III) flumequine and (C): Sm(III) flumequine complexes

Three absorption bands at 233, 249, and 321 nm in the UV–Vis spectrum of the FLQ free drug ligand (Figure 1S, supplementary file) are attributed to charge–transfer, $\pi\rightarrow\pi^*$, and $n\rightarrow\pi^*$ transitions, respectively [43]. The electronic absorption spectra of $[La(FLQ)_2(Cl)(H_2O)].3H_2O$, $[Sm(FLQ)_2(Cl)(H_2O)]$, $[Tb(FLQ)_2(Cl)(H_2O)].2H_2O$ complexes are located at 226-231 nm, 245-248 nm, and 312-317 nm, respectively. These bands are caused by electronic transitions of charge-transfer, $\pi\rightarrow\pi^*$ and $n\rightarrow\pi^*$.

Table 2. FT-IR frequencies (cm^{-1}) and their assignments for FLQ drug and its complexes.

FLQ	La(III) complex	Tb(III) complex	Sm(III) complex	Assignments
1725	-	-	-	ν(C=O); COOH
1617	1627	1640	1646	ν(C=O); pyridone ring
-	1569	1598	1598	ν_{as}(COO)
-	1374	1375	1384	ν_s(COO)
1267	1257	1257	1257	ν(C-O); COO group
-	195	223	214	$\Delta\nu = [\nu_{as}(COO) - \nu_s(COO)]$
-	488, 409	478, 448	478, 448	ν(M-O)

Thermal analyses

Thermal analysis was operated at 10 ºC/min heating rates under nitrogen environment in temperature range from 25-to-600 ºC (Figure 4). The thermal degradation of flumequine drug ligand has two endothermic steps.

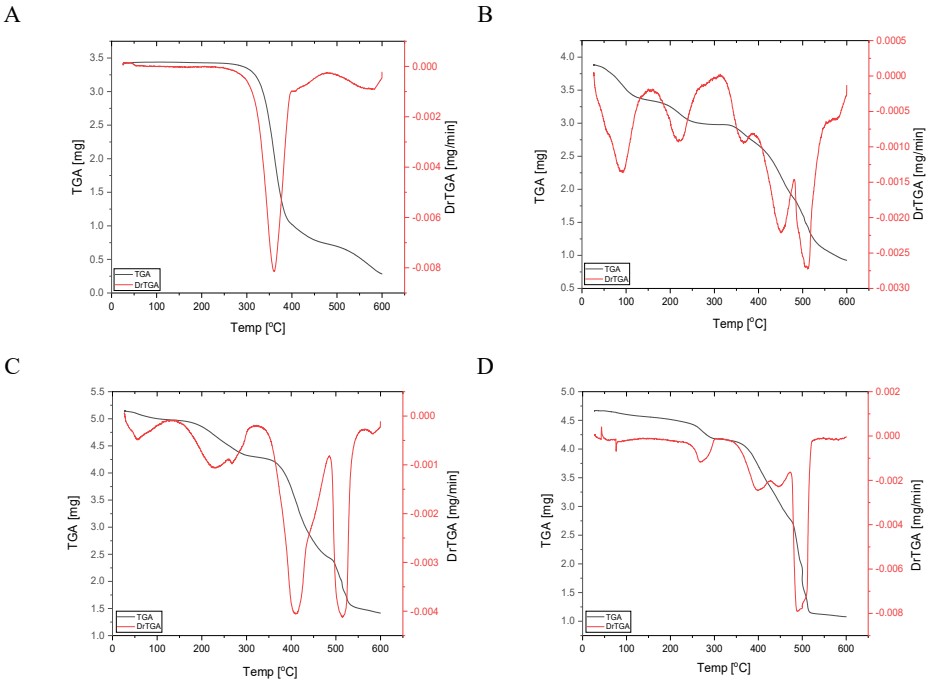

Figure 4. TGA and DTG curves of (A): flumequine free ligand, (B): La(III) flumequine, (C): Tb(III) flumequine and (D): Sm(III) flumequine complexes.

The first stage take place at the maximum temperature of 360 ºC, the second decomposition step occurs at a maximum temperature of 570 ºC. Few carbon unoxidized remains as residual product at 800 ºC. The $[La(FLQ)_2(Cl)(H_2O)].3H_2O$ complex take place in five degradation stages. The first stage of decomposition occurs at maximum temperature of 89 ºC associated with release of $3H_2O$ uncoordinated molecules. The decomposition from two-to-five stages occurs at the maximum temperatures 221, 367, 450 and 510 ºC, respectively. The weight losses at these steps associated with the loss ($½Cl_2$+H_2O+2FLQ ligand molecules). The FTIR spectrum of the final thermal decomposition product, $½La_2O_3$ of this complex was checked. The thermal decomposition of the $[Tb(FLQ)_2(Cl)(H_2O)].2H_2O$ complex is take place in four degradation stages. The first stage of decomposition occurs at maximum temperature of 54 ºC. The weight loss associated with this step may be attributed to loss of two uncoordinated water molecules. The decomposition from two-to-four stages occurs at the maximum temperatures 230, 410 and 515 ºC, respectively. The weight losses at these steps associated with the loss one water molecule + one chlorine coordinated atom and two molecules of flumequine (FLQ) ligand. The final thermal decomposition product, $½Tb_2O_3$. The thermal decomposition of $[Sm(FLQ)_2(Cl)(H_2O)]$ complex proceeds with four degradation stages. The first stage of decomposition occurs at maximum

temperature of 267 °C. The weight loss associated with this step may be attributed to loss of one coordinated water molecule and one coordinated chlorine atom. The decomposition from two-to-four stages occurs at the maximum temperatures 397, 444 and 490 °C, respectively. The weight losses at these steps associated with the loss two coordinated molecules of flumequine (FLQ) ligand. The final thermal decomposition product, ½Sm_2O_3.

XRD, SEM and EDX studies

The X-ray powder diffraction patterns of [La(FLQ)$_2$(Cl)(H_2O)].3H_2O, [Sm(FLQ)$_2$(Cl) (H_2O)], [Tb(FLQ)$_2$(Cl)(H_2O)].2H_2O complexes are shown in Figure 5. The generated complexes' X-ray pattern diffractions show a variety of reflections in a highly crystalline phase. The Debye-Scherrer formula (Eq. 1) [44] was utilized to compute the average crystallite size (D). The wavelength of the X-ray is λ, which is equal to 1.5418 Å for Cu Kα radiation. The full width at half maximum (FWHM) of the prominent intensity peak is β, which is 100% relative intensity peak. The peak position is θ and K is assumed to be constant at 0.94. The estimated grain sizes for the La(III), Sm(III), and Tb(III) complexes were determined to be 37, 24, and 36 nm, respectively, using the Debye-Scherrer formula. The growing amount of chelates surrounding metal ions can be used to explain the smaller grain size of complexes [45]. Using the relation (Eq. 2), the strain (ε) was determined from the slope of the β cos θ against sin θ plot. Reductions in strain and dislocation density signify the creation of high-quality complexes since they are the outward expressions of the dislocation network within the complexes. Table 3 displays the dislocation density (δ), which was calculated using Eq. 3 [46]:

$$D = \frac{K\,\lambda}{\beta \cos\theta} \tag{1}$$

$$\beta = \frac{\lambda}{D \cos\theta} - \varepsilon \tan\theta \tag{2}$$

$$\delta = \frac{1}{D^2} \tag{3}$$

Table 3. Data of 2-theta, intensity, d-spacing, crystallite sizes (D), dislocation density (δ), and strain (ε).

Complexes	2-theta	Intensity	D (nm)	δ (10^{12}.lin.m^{-2})	ε (10^{-4})
La(III)	33	4749	37	0.0007	0.6470
Sm(III)	17	675	24	0.0017	1.9257
Tb(III)	16	3300	36	0.0008	1.3658

The solid complexes of [La(FLQ)$_2$(Cl)(H_2O)].3H_2O, [Sm(FLQ)$_2$(Cl)(H_2O)], [Tb(FLQ)$_2$(Cl)(H_2O)].2H_2O are seen in scanning electron microscope pictures (Figure 6). Using the SEM technique, the morphological phases for the scanned La(III), Sm(III), and Tb(III) complexes were checked. The SEM pictures (Figure 6A–C) are of the uniform size. Depending on the size and form of the aggregation, the nano-sized particles of the produced complexes are present quite close to one another [47]. Utilizing EDX data, the percentage level of components contained in the FLQ-lanthanide complexes was ascertained (Figure 6A-C).

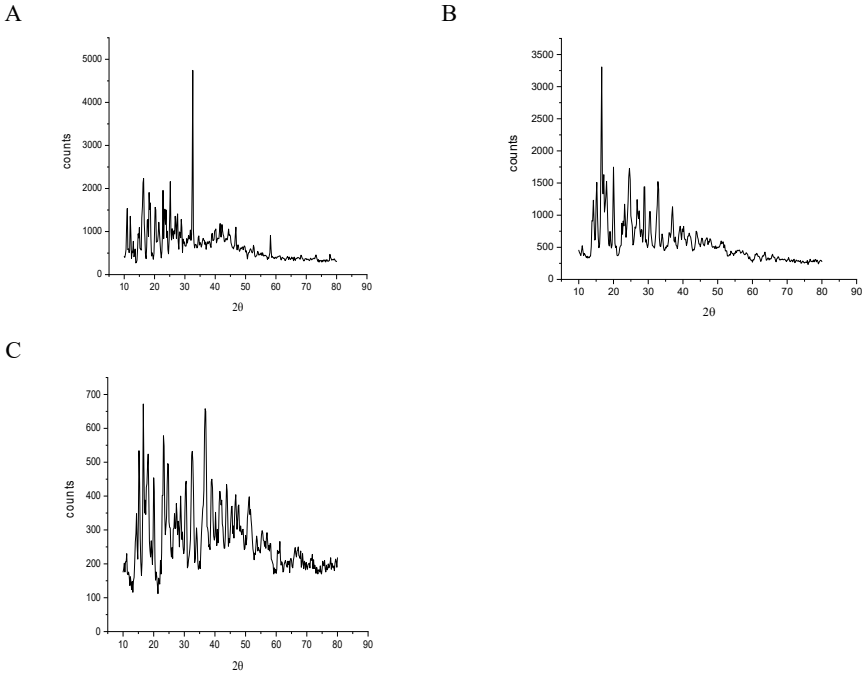

Figure 5. XRD spectra of (A): La(III) flumequine, (B): Tb(III) flumequine and (C): Sm(III) flumequine complexes.

Anticancer assessments

The cytotoxic activity of the metal complexes $[La(FLQ)_2(Cl)(H_2O)].3H_2O$, $[Sm(FLQ)_2(Cl)(H_2O)]$, $[Tb(FLQ)_2(Cl)(H_2O)].2H_2O$ was evaluated against human liver HepG2 cancer cell, (HepG2 cell line) and MCF-7 cells (human breast cancer cell line) within 0.0–500 µg/mL concentration range. The IC_{50} values were calculated for each complex and results are presented in Figure 7A&B. As shown, most complexes displayed significantly cytotoxic activities compared to cis-platinum standard drug. It seems that the nature of the metal ion has effect on the biological behaviour. Cytotoxicity activity of the complexes may be attributed to the central metal atom which was explained by Tweedy's chelation theory [48]. Cytotoxicity results indicated that all tested complexes cytotoxicity evaluation of La(III) (IC_{50} = 58.2 ± 3.1 µg/mL), Tb(III) (IC_{50} =199 ± 6.7 µg/mL), and Sm(III)-FLQ (IC_{50} = 95.7 ± 4.9 µg/mL) complexes against HepG-2 cell line. The cytotoxicity evaluation of La(III) (IC_{50} = 61.5 ± 3.8 µg/mL), Tb(III) (IC_{50} = 215 ± 8.4 µg/mL), and Sm(III)-FLQ (IC_{50} = 115 ± 6.3 µg/mL) complexes against MCF-7 cell line. The enhancement of cytotoxic activity may be assigned to that the positive charge of the metal increased the acidity of coordinated ligand that bears protons, leading to stronger hydrogen bonds which enhanced the biological activity [48].

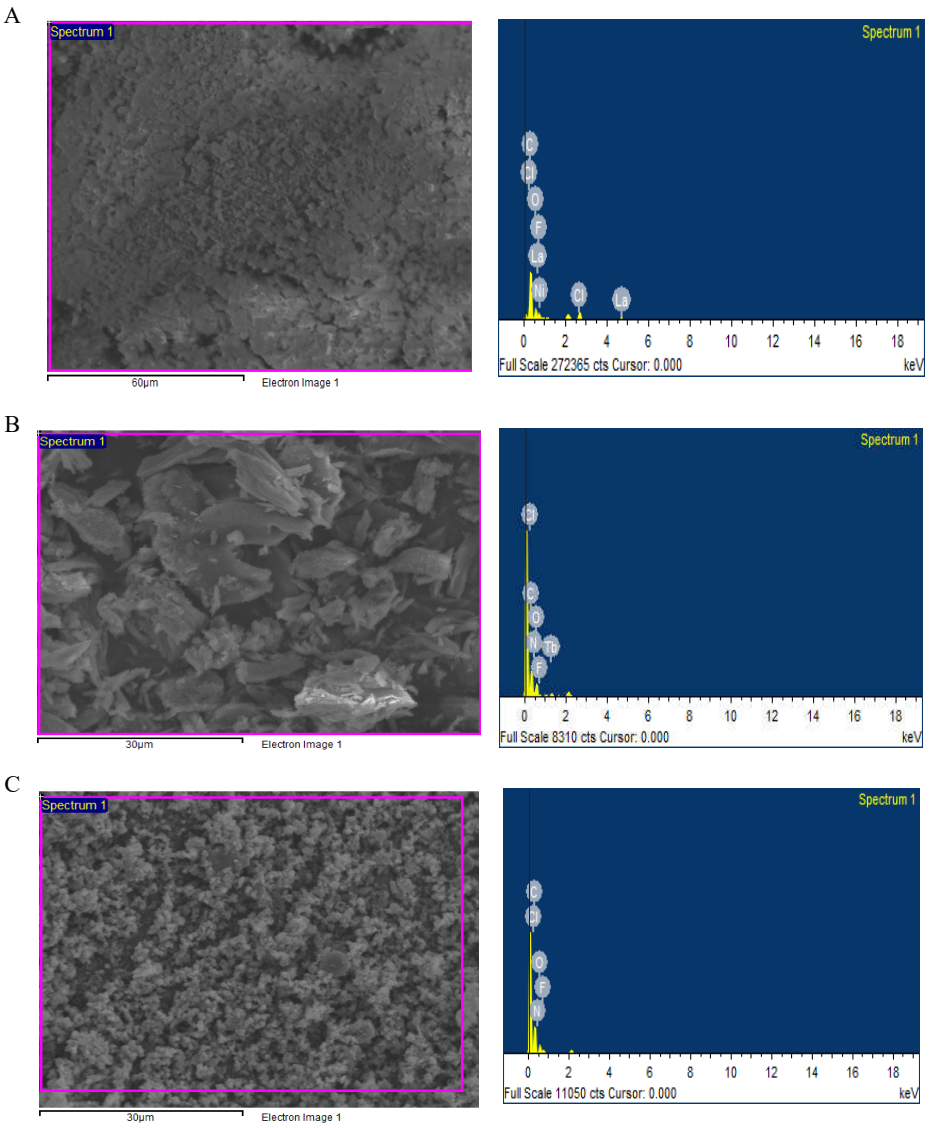

Figure 6. SEM images and EDX spectra of (A): La(III) flumequine, (B): Tb(III) flumequine and (C): Sm(III) flumequine complexes.

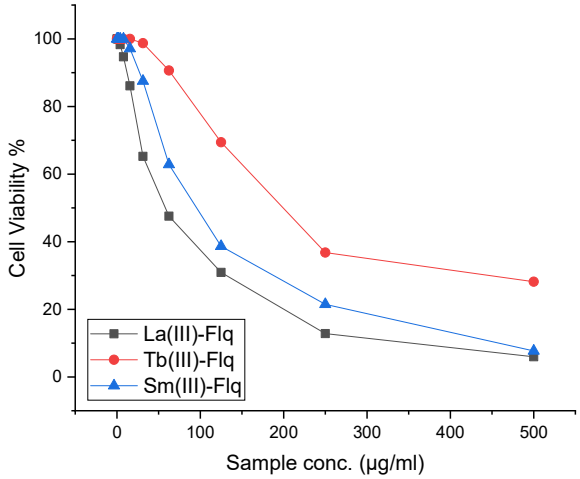

Figure 7A. Curves of cytotoxicity evaluation of La(III) (IC_{50} = 58.2 ± 3.1 µg/mL), Tb(III) (IC_{50} =199 ± 6.7 µg/mL), Sm(III)-FLQ (IC_{50} = 95.7 ± 4.9 µg/mL) complexes against HepG-2 cell line.

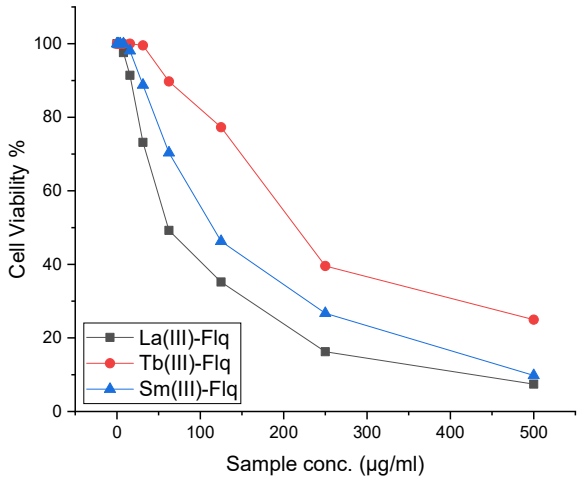

Figure 7B. Curves of cytotoxicity evaluation of La(III) (IC_{50} = 61.5 ± 3.8 µg/mL), Tb(III) (IC_{50} = 215 ± 8.4 µg/mL), Sm(III)-FLQ (IC_{50} = 115 ± 6.3 µg/mL) complexes against MCF-7 cell line.

CONCLUSION

In the current work, flumequine drug ligand was used to create three novel metal nanostructured complexes. The development of these three metal nanostructured complexes was confirmed by SEM analysis, FTIR, TGA, powder XRD, and UV/Vis spectroscopy used to characterize the

complexes. $[M(FLQ)_2(Cl)(H_2O)].nH_2O$ type complexes are made up of all metal complexes. IR spectra, analytical data, and thermal analysis, the geometries attributed to La(III), Sm(III) and Tb(III) are octahedral shape. The creation of bonds in all these complexes involves the oxygen carboxylic, and carbonyl oxygen. The metal complexes show remarkable pharmacology due to their strong anticancer effect. Cytotoxicity evaluation of La(III) (IC_{50} = 58.2 ± 3.1 µg/mL), Tb(III) (IC_{50} =199 ± 6.7 µg/mL), Sm(III)-FLQ (IC_{50} = 95.7 ± 4.9 µg/mL) complexes against HepG-2 cell line and the cytotoxicity evaluation of La(III) (IC_{50} = 61.5 ± 3.8 µg/mL), Tb(III) (IC_{50} = 215 ± 8.4 µg/mL), Sm(III)-FLQ (IC_{50} = 115 ± 6.3 µg/mL) complexes against MCF-7 cell line. As a result, they can be applied even more to useful drug action research.

ACKNOWLEDGEMENT

Princess Nourah bint Abdulrahman University Researchers Supporting Project number (PNURSP2024R75), Princess Nourah bint Abdulrahman University, Riyadh, Saudi Arabia.

REFERENCES

1. Turel, I. The interactions of metal ions with quinolone antibacterial agents. *Coord. Chem. Rev*. **2002**, 232, 27-47.
2. Wagman, A.S.; Wentland, M.P. *Comprehensive Medicinal Chemistry II*, Vol. 7, Tayler, J.B.; Triggle, D.J. (Eds.), Elsevier Ltd.: Amsterdam; **2007**, pp. 567-596.
3. Andriole, V.T. The quinolones: Past, present, and future. *Clin. Infect. Dis.* **2005**, 41, S113-S119.
4. Turel, I. The interactions of metal ions with quinolone antibacterial agents. *Coord. Chem. Rev*. **2002**, 232, 27-47.
5. Bashir, M.; Yousuf, I. Synthesis, structural characterization and *in vitro* cytotoxic evaluation of mixed Cu(II)/Co(II) levofloxacin–bipyridyl complexes. *Inorg. Chim. Acta* **2022**, 532, 120757.
6. Heberer, T. Occurrence, fate, and removal of pharmaceutical residues in the aquatic environment: A review of recent research data. *Toxicol. Lett*. **2002**, 131, 5-17.
7. Ternes, T.A. Occurrence of drugs in German sewage treatment plants and rivers. *Water Res*. **1998**, 32, 3245-3260.
8. Steer, C.R.; Huby, C.L.; Ball, A.P.; Dickinson, R.J.; Pickens, S.; Wallace, E.T.; Wilson, A.M.M.; Gray, J.A. Clinical and laboratory studies with R802, a new synthetic quinolone, in urinary tract infection. *J. Antimicrob. Chemother*. **1981**, 7, 643-648.
9. Rohlfing, S.R.; Gerster, J.F.; Kvam, D.C. Bioevaluation of the antibacterial flumequine for urinary tract use. *Antimicrob. Agents Chemother*. **1976**, 10, 20-24.
10. Alghamdi, M.T.; Alsibaai, A.A.; Shahawi, M.S.; Refat, M.S. Synthesis and spectroscopic studies of levofloxacin uni-dentate complexes of Ru(III), Pt(IV) and Ir(III): Third generation of quinolone antibiotic drug complexes. *J. Mol. Liq*. **2016**, 224, 571-579.
11. King, D.E.; Malone, R.; Lilley, S.H. New classification and update on the quinolone antibiotics. *Am. Fam. Physician* **2000**, 61, 2741-2748.
12. Crisponi, G.; Nurchi, V.M.; Fanni, D.; Gerosa, C.; Nemolato, S.; Faa, G. Copper-related diseases: From chemistry to molecular pathology. *Coord. Chem. Rev*. **2010**, 254, 876-889.
13. Drewry, J.A.; Gunning, P.T. Recent advances in biosensory and medicinal therapeutic applications of zinc(II) and copper(II) coordination complexes. *Coord. Chem. Rev*. **2011**, 255, 459-472.
14. Sorenson, J.R.J. 6 copper complexes offer a physiological approach to treatment of chronic diseases. *Prog. Med. Chem.* **1989**, 26, 437-568.

15. Weder, J.E.; Dillon, C.T.; Hambley, T.W.; Kennedy, B.J.; Lay, P.A.; Biffin, J.R.; Regtop, H.L.; Davies, N.M. Copper complexes of non-steroidal anti-inflammatory drugs: an opportunity yet to be realized. *Coord. Chem. Rev*., **2002**, 232, 95-126.
16. Efthimiadou, E.K.; Thomadaki, H.; Sanakis, Y.; Raptopoulou, C.P.; Katsaros, N.; Scorilas, A.; Karaliota, A.; Psomas, G. Copper complexes of non-steroidal anti-inflammatory drugs: an opportunity yet to be realized. *J. Inorg. Biochem*. **2007**, 101, 64-73.
17. Katsarou, M.E.; Efthimiadou, E.K.; Psomas, G.; Karaliota, A.; Vourloumis, D. Novel copper(II) complex of N-propyl-norfloxacin and 1,10-phenanthroline with enhanced antileukemic and DNA nuclease activities. *J. Med. Chem*. **2008**, 51, 470-478.
18. Dimiza, F.; Fountoulaki, S.; Papadopoulos, A.N.; Kontogiorgis, C.A.; Tangoulis, V.; Raptopoulou, C.P.; Psycharis, V.; Terzis, A.; Kessissoglou, D.P.; Psomas, G. Non-steroidal antiinflammatory drug–copper(II) complexes: Structure and biological perspectives. *Dalton Trans*. **2011**, 40, 8555-8568.
19. Dimiza, F.; Perdih, F.; Tangoulis, V.; Turel, I.; Kessissoglou, D.P.; Psomas, G. Interaction of copper(II) with the non-steroidal anti-inflammatory drugs naproxen and diclofenac: synthesis, structure, DNA-and albumin-binding. *J. Inorg. Biochem*. **2011**, 105, 476-489.
20. Ruiz, M.; Perello, L.; Server-Carrio, J.; Ortiz, R.; Garcia-Granda, S.; Diaz, M.R.; Canton, E. Cinoxacin complexes with divalent metal ions. Spectroscopic characterization. Crystal structure of a new dinuclear Cd(II) complex having two chelate-bridging carboxylate groups. Antibacterial studies. *J. Inorg. Biochem.* **1998**, 69, 231-239.
21. Hueso-Urena, F.; Moreno-Carretero, M.N.; Romero-Molina, M.A.; Salas-Peregrin, J.M.; Sanchez-Sanchez, M.P.; Alvarez de Cienfuegos-Lopez, G.; Faure, R. Transition metal complexes with monodeprotonated isoorotic and 2-thioisoorotic acids: Crystal structure, spectral and magnetic study, and antimicrobial activity. *J. Inorg. Biochem.* **1993**, 51, 613-632.
22. Saha, D.K.; Sandbhor, U.; Shirisha, K.; Padhye, S.; Deobagkar, D.; Anson, C.E.; Powell, A.K. A novel mixed-ligand antimycobacterial dimeric copper complex of ciprofloxacin and phenanthroline. *Bioorg. Med. Chem. Lett*. **2004**, 14, 3027-3032.
23. Ramadan, A.M. Structural and biological aspects of copper(II) complexes with 2-methyl-3-amino-(3 *H*)-quinazolin-4-one. *J. Inorg. Biochem*. **1997**, 65, 183-189.
24. Asadpour, S.; Aramesh-Boroujeni, Z.; Jahani, S. In vitro anticancer activity of parent and nano-encapsulated samarium(III) complex towards antimicrobial activity studies and FS-DNA/BSA binding affinity. *RSC adv.* **2020**, 10, 31979-31990.
25. Aramesh-Boroujeni, Z.; Aramesh, N.; Jahani, S.; Khorasani-Motlagh, M.; Kerman, K.; Noroozifar, M. Experimental and computational interaction studies of terbium(III) and lanthanide(III) complexes containing 2,2′-bipyridine with bovine serum albumin and their in vitro anticancer and antimicrobial activities. *J. Biomol. Struct. Dyn*. **2021**, 39, 5105-5116.
26. He, X.Q.; Lin, Q.Y.; Hu, R.D.; Lu, X.H. Synthesis, characterization and DNA-binding studies on La(III) and Ce(III) complexes containing ligand of *N*-phenyl-2-pyridinecarboxamide. *Spectrochim. Acta Part A* **2007**, 68, 184-190.
27. Bao, Z.; Lai, D.; Shen, P.; Yu, M.; Kumar, R.; Liu, Y.; Liang, H. A new samarium(III) complex of liriodenine: Synthesis, crystal structure, antitumor activity, and DNA binding study. *Zeitschrift für Anorganische Und Allgemeine Chemie* **2019**, 645, 570-579.
28. Xu, D.; Ma, S.; Du, G.; He, Q.; Sun, D. Synthesis, characterization, and anticancer properties of rare earth complexes with Schiff base and *o*-phenanthroline. *J. Rare Earth* **2008**, 26, 643-647.
29. Teo, R.D.; Termini, J.; Gray, H.B. Lanthanides: Applications in cancer diagnosis and therapy. *J. Med. Chem*. **2016**, 59, 6012-6024.
30. Liu, Y.C.; Chen, Z.F.; Song, X.Y.; Peng, Y.; Qin, Q.P.; Liang, H. Synthesis, crystal structure, cytotoxicity and DNA interaction of 5,7-dibromo-8-quinolinolato-lanthanides. *Eur. J. Med. Chem*. **2013**, 59, 168-175.

31. Ruiz-Garcia, A.; Bermejo, M.; Merino, V.; Sanchez-Castano, G.; Freixas, J.; Garrigues, T.M.; Pharmacokinetics, bioavailability and absorption of flumequine in the rat. *Eur. J. Pharm. Biopharm*. **1999**, 48, 253-258.
32. Delmas, J.M.; Chapel, A.M.; Sanders, P. Determination of flumequine and 7-hydroxyflumequine in plasma of sheep by high-performance liquid chromatography. *J. Chromatogr. B: Biomed. Sci. Appl*. **1998**, 712, 263-268.
33. Skyrianou, K.C.; Perdih, F.; Turel, I.; Kessissoglou, D.P.; Psomas, G. Nickel–quinolones interaction: Part 3-Nickel(II) complexes of the antibacterial drug flumequine. *J. Inorg. Biochem*. **2010**, 104, 740-749.
34. Chalkidou, E.; Perdih, F.; Turel, I.; Kessissoglou, D.P.; Psomas, G. Copper(II) complexes with antimicrobial drug flumequine: Structure and biological evaluation. *J. Inorg. Biochem*. **2012**, 113, 55-65.
35. Tarushi, A.; Kljun, J.; Turel, I.; Pantazaki, A.A.; Psomas, G.; Kessissoglou, D.P. Zinc(II) complexes with the quinolone antibacterial drug flumequine: Structure, DNA-and albumin-binding. *New J. Chem.* **2013**, 37, 342-355.
36. Tsitsa, I.; Tarushi, A.; Doukoume, P.; Perdih, F.; De Almeida, A.; Papadopoulos, A.; Kalogiannis, S.; Casini, A.; Turel, I.; Psomas, G. Structure and biological activities of metal complexes of flumequine. *RSC Adv.* **2016**, 6, 19555-19570.
37. Mosmann, T. Rapid colorimetric assay for cellular growth and survival: application to proliferation and cytotoxicity assays. *J. Immunol. Methods* **1983**, 65, 55-63.
38. Gomha, S.M.; Riyadh, S.M.; Mahmmoud, E.A.; Elaasser, M.M. Synthesis and anticancer activities of thiazoles, 1,3-thiazines, and thiazolidine using chitosan-grafted-poly(vinylpyridine) as basic catalyst. *Heterocycles* **2015**, 91, 1227-1243.
39. Refat, M.S. Synthesis and characterization of ligational behavior of curcumin drug towards some transition metal ions: Chelation effect on their thermal stability and biological activity. *Spectrochim. Acta Par A* **2013**, 105, 326-337.
40. Nakamoto, K. *Infrared Spectra of Inorganic and Coordination Compounds*, 2nd ed., Wiley Interscience: New York; **1970**.
41. Bellamy, L.J. *The Infrared Spectra of Complex Molecules*, Chapman and Hall: London; **1975**.
42. Deacon, G.B.; Phillips, R. Relationships between the carbon-oxygen stretching frequencies of carboxylato complexes and the type of carboxylate coordination. *Coord. Chem. Rev*. **1980**, 33, 227-250.
43. Lever, A.B. *Inorganic Electronic Spectroscopy*, Elsevier: Amsterdam; **1968**.
44. Cullity, B.D. *Elements of X-Ray Diffraction*, Addison-Wesley: Reading, MA; **1972**; p. 102.
45. Salavati-Niasari, M.; Mohandes, F.; Davar, F.; Mazaheri, M.; Monemzadeh, M.; Yavarinia, N. Preparation of NiO nanoparticles from metal-organic frameworks via a solid-state decomposition route. *Inorg. Chim. Acta* **2009**, 362, 3691-3697.
46. Velumani, S.; Mathew, X.; Sebastian, P.J. Structural and optical characterization of hot wall deposited CdSe*x*Te1−*x* films. *Solar Energy Mater. Solar Cells* **2003**, 76, 359-368.
47. Carotenuto, G.; Nicolais, F.; Reversible thermochromic nanocomposites based on thiolate-capped silver nanoparticles embedded in amorphous polystyrene. *Materials* **2009**, 2, 1323-1340.
48. Ramadan, A.M. Structural and biological aspects of copper(II) complexes with 2-methyl-3-amino-(3H)-quinazolin-4-one. *J. Inorg. Biochem*. **1997**, 65, 183-189.